Determination of the titanium spectral function from (e,e'p) data from Jefferson Lab E12-14-012 experiment

Albrun Johnson[1] and Camillo Mariani[2]

[1]*Department of Physics, Gettysburg College, Gettysburg, Pennsylvania 17325, USA*
[2]*Center for Neutrino Physics, Virginia Tech, Blacksburg, Virginia 24061, USA*

The experiment E12-14-012 at Thomas Jefferson National Accelerator Facility (JLab) gathered data from (e,e'p) scattering on a titanium-48 natural target. The (e,e'p) cross section was extracted as a function of the missing momentum p_m and the missing energy E_m, respectively, to get the titanium proton spectral functions and the spectroscopic factors. The measurements were then fitted against a Monte Carlo simulation varying orbitals' strength, position and width, and the reduced χ^2 values were determined using TMinuit in ROOT. The fitting procedure was performed with and without the correlated part of the spectral function for both the p_m and E_m fits, and, the latter, with and without including the results on spectroscopic factors obtained from the p_m fits. There was no significant difference between using or not using the correlated spectral function for the p_m fits but the reduced χ^2 value was closer to 1 at 0.57 when not using it. For the E_m fits, there was no significant difference between using all priors and not using the p_m fits fits but there was a slight difference to not using the correlated spectral function. The reduced χ^2 value was best when using all priors at 0.95. Neither fit shows a bias and while the p_m fits should be run without the correlated spectral function, the E_m fits should be run with all priors to obtain the best fit.

I. INTRODUCTION

The Deep Underground Experiment (DUNE) will study neutrino oscillation to gain insight on the origin of matter, the relationship between the four forces, and black hole formation, among other fields. Specifically, DUNE will look at ν_μ to ν_e and $\bar{\nu_\mu}$ to $\bar{\nu_e}$ oscillation. The idea behind measuring neutrino oscillation with higher precision is to test the validity of the three-flavor paradigm and in the process check for charge-parity symmetry violation. DUNE's infrastructure can also be used to detect rare supernova neutrino bursts, and nucleon decay and neutron-antineutron oscillations, which if observed would be evidence for baryon-number violation. DUNE will consist of a near detector, a far detector, and a neutrino beam-line. The neutrino source and the near detector will be located at Fermi National Accelerator Laboratory (Fermilab) in Illinois. For the beam-line, protons will be accelerated and will collide with a graphite target. The resulting pions and kaons will either decay into ν_μ and $\bar{\nu_\mu}$ or be filtered out with the use of a pulsating horn. The near detector complex will measure the neutrinos and antineutrinos before oscillation and will be used to reduce the systematic error due to neutrino cross section and nuclear models. The near detector includes on-axis and off-axis neutrino detectors. The far detector will be located 850 miles from Fermilab at Sanford Underground Research Facility (SURF) in South Dakota approximately 1,500 m underground. The far detector will consist of four liquid argon time-projection chamber modules with a volume of about 17 kt [1–3].

In the DUNE detectors, the neutrinos and antineutrinos will interact with argon-40 nuclei. Since the energy of the incoming neutrinos will not be known precisely (neutrinos come from 3-body decay of pions and kaons), it is essential to understand the nuclear structure of argon to reconstruct the neutrino energy from the product of the neutrino interactions in the detectors. The energy of the incoming neutrino is necessary to determine the oscillation probability:

$$P(\nu_\alpha \to \nu_\beta) \simeq \sin^2 2\theta \sin^2\left(\frac{\Delta m^2 L}{4E}\right), \tag{1}$$

where θ is the mixing angle, δm is the squared difference in neutrino mass, L is the oscillation distance (far-near detector), and E is the reconstructed (anti-)neutrino energy. For simplicity, this probability only incorporates two neutrino flavors instead of three. While we can find argon's proton spectral function using the (e,e'p) cross section, (e,e'n) scattering is not efficient - the cross section is about 10% of the (e,e'p) cross section and with a typical neutron efficiency of 50%, the total cross section is about 5%. Hence (e,e'n) is not well suited for determining argon's neutron spectral function with very high statistics. Instead, we used (e,e'p) scattering in titanium-48 to model the neutron spectral function as the protons' structure in titanium is quite similar to the neutrons in argon. There are differences of course, one being the additional eight neutrons in titanium wit respect to the argon's protons [5]. The theory group of Barbieri in Ref. [4] has shown that this is a viable model for inclusive (e,e') scattering, suggesting that this approximation may work also for the exclusive scattering.

In the E12-14-012 experiment we use an electron beam of energy 2.222 GeV produced by the CEBAF accelerator and it was aimed at gaseous closed argon cell and a solid titanium target, respectively. The resulting particles were detected using an electron and a proton spectrometers. The difference in momentum and energy in the interaction are the missing momentum p_m and the missing energy E_m given by

$$\mathbf{p}_m = \mathbf{q} + \mathbf{p}' = \mathbf{p}_R \tag{2}$$

and

$$E_m = \omega - T_{p'} - T_R, \tag{3}$$

where $\mathbf{q}$ is the momentum transfer, $\mathbf{p}'$ the outgoing proton's momentum, $\mathbf{p}_R$ the momentum of the recoiling residual nucleus, ω the energy transfer, $T_{p'}$ the outgoing proton's kinetic

TABLE I. Kinematics settings used to collect the data in experiment E12-14-012.

	E'_e (GeV)	θ_e (deg)	Q^2 (GeV$^2/c^2$)	$\|\mathbf{p}'\|$ (MeV/c)	$T_{p'}$ (MeV)	$\theta_{p'}$ (deg)	$\|\mathbf{q}\|$ (MeV/c)	p_m (MeV/c)	E_m (MeV)
kin1	1.799	21.5	0.549	915	372	−50.0	865	50	50
kin2	1.716	20.0	0.460	1030	455	−44.0	846	184	50
kin3	1.799	17.5	0.370	915	372	−47.0	741	174	50
kin4	1.799	15.5	0.291	915	372	−44.5	685	230	50

energy, and T_R is the kinetic energy of the recoiling nucleus. The four different kinematics that were used for titanium are shown in Table I. The angle of the incoming electron beam was changed to sample different missing momentum [5]. Using the data from the experiment we measured the (e,e′p) cross section

$$\frac{d^6\sigma}{d\omega d\Omega_{e'} dT_{p'} d\Omega_{p'}} = \frac{Y(p_m, E_m)}{B \times lt \times \rho \times V_B \times C_{\text{rad}}}, \tag{4}$$

where B is the total accumulated beam charge, lt is the live-time of the detector, ρ is the target density, V_B is the effect of the acceptance and kinematical cuts, and C_{rad} is the effect of the radiative corrections and bin center migration. The cross section is

$$\frac{d^6\sigma_{IA}}{d\Omega_{e'} d E_{e'} d\Omega_{p'} d E_{p'}} \propto \sigma_{ep} P(p_m, E_m) T(E_{p'}), \tag{5}$$

where σ_{ep} is the elementary cross section, $P(p_m, E_m)$ is the spectral function - which consists to 80% of the mean field and to 20% of the correlated part - and $T(E_{p'})$ is the FSI effects, as functions of p_m and E_m, respectively. By dividing out the FSI and the elementary cross section - using de Forest's σ_{CC1} for the off-shell proton cross section [6, 7] - we obtained $P(p_m)$ and its corresponding spectroscopic factors S_α. Using the spectroscopic factors from the p_m fit and the cross section as a function of E_m, we found $P(E_m)$ and its parameters - the spectroscopic factors, the peak positions, and the distribution width. We fitted these values against a Monte Carlo simulation (MC) to test for bias and determine the best fit. The MC simulation used the SIMC spectrometer package to simulate the (e,e′p) events. It operates with the kinematic settings from the experiment and an approximate spectral function as input, built assuming the independent shell model [8, 13].

II. DATA ANALYSIS

We used the CERN ROOT package to find the best fit for p_m and E_m and in them the ROOT TMinuit package to minimize χ^2. TMinuit takes the parameters given by the user and finds the value in a determined interval to find the smallest χ^2 value [14, 15]. We calculated χ^2 with

$$\chi^2 = \sum_i \chi_i^2 = \sum_i \left(\frac{\sigma_i^{\text{red, obs}} - \sum_\alpha S_\alpha f_\alpha^{\text{pred}}(i)}{\sigma_{\sigma_i^{\text{red, obs}}}} \right)^2, \tag{6}$$

where $\sigma_i^{\text{red, obs}}$ is the observed, reduced cross section, the index i labels the missing momentum bin, α is the orbital index, $f_\alpha^{\text{pred}}(i)$ is the parametrized prediction evaluated at bin i in the missing momentum spectra for orbital α, and S_α is the spectroscopic factor. We minimized the χ^2 function using the missing energy spectra,

$$\chi^2 = \sum_i \chi_i^2 + \sum_n \left(\frac{\tau_n^{\text{fit}} - \tau_n^c}{\sigma_n^{\text{fit}}} \right)^2, \tag{7}$$

including constraints from previous experimental results [9–12], summarized in Table III. For comparison, we normalized χ^2 by dividing by the number of degree of freedom (d.o.f.) which is known as the reduced χ^2 value. The d.o.f is defined as the number of fitted parameters minus the number of independent values (including constraints). If the reduced χ^2 value is one, it fits the data perfectly; if it is higher, the data does not match the fit well; and if it is lower, it could be an indication that the data is either over fitted or the errors are overestimated.

The p_m fit used 9 fitting parameters, while the E_m fit used 25. We ran both fitting codes with and without the correlated part of the spectral function to determine possible bias on the spectroscopic factors due to the assumptions used to compute the correlated part of the spectral function [13].

In the E_m fit, we looked at the fit results including or not the constraints on spectroscopic factor obtained by the p_m fit. In both cases, we determined the peak energy positions and their distribution widths. This process tests the fit for bias in determining the spectral function. The spectroscopic factors in Table IV and Table V were normalized to 0.8×22 for the total strength of the orbitals and to 0.2×22 for the correlated part. The total spectroscopic strength, which is the sum of the spectroscopic factors of the individual orbitals and the correlated part, should be at 22 as the total number of protons in titanium. The error is a combination of systematic and statistical uncertainty as summarized in Table II. We used the procedure outlined in Ref. [13] to determine the errors.

III. RESULTS

Figure 1 shows the p_m distributions of the four kinematics integrated over three different E_m intervals. The dots represent our data points, their errors, that consists of the systematic and statistical errors summed in quadrature, and the theoretical model is the blue band. Further uncertainties in the theoretical model (like the effect of FSI) are included in the width of the blue band. It is notable that kinematics two and three cover

TABLE II. Contributions to systematical uncertainties for titanium average over all the E_m and p_m bins for each kinematic. All numbers are in %. kin4 uncertainties are the sum in quadrature of the systematic uncertainties on the signal and the background.

	kin1	kin2	kin3	kin4
1. Total statistical uncertainty	0.78	0.60	0.82	1.24
2. Total systematic uncertainty	4.63	4.92	4.70	6.04
a. Beam $x\&y$ offset	0.49	1.17	0.66	0.91
b. HRS $x\&y$ offset	0.58	1.25	0.99	1.15
c. Optics (q1, q2, q3)	0.48	0.77	0.55	0.90
d. Acceptance cut (θ, ϕ, z)	1.36	1.46	1.32	1.57
e. Target thickness/density/length	0.20	0.20	0.20	0.20
f. Calorimeter & Čerenkov cut	0.02	0.02	0.02	0.02
g. Radiative and Coulomb corr.	1.00	1.00	1.00	1.00
h. β cut	0.39	0.58	0.42	2.83
i. Cross section model	1.00	1.00	1.00	1.00
j. Trigger and coincidence time cut	0.78	0.33	0.58	2.32
k. FSI	4.00	2.00	2.00	2.00

TABLE III. Constraints on the fits to the missing-energy spectra obtained from past measurements [9–12]. For the clarity of presentation, E_α is denoted as $E(\alpha)$.

Parameter	Value (MeV)	Uncertainty (MeV)
$E(1f_{7/2})$	11.32	0.10
$E(1d_{3/2})$	12.30	0.24
$E(2s_{1/2})$	12.77	0.25
$E(1d_{5/2})$	15.86	0.20
$E(1d_{5/2}) - E(1d_{3/2})$	3.57	0.31
$E(1p_{3/2}) - E(1p_{1/2})$	6.36	0.75

the same region in p_m but have different $T_{p'}$, so the effect of final state interactions (FSI) between them is different. The quite good agreement in the reduced cross section shows that our FSI corrections are reliable.

The total spectroscopic strengths, obtained with and without the use of the correlated spectral function in Table IV, match within uncertainty at 22.16 ± 5.31 and 20.17 ± 4.14, respectively. There is no significant difference for the individual spectroscopic factors except in the $1s_{1/2}$ shell but the difference is not big. The reduced χ^2 value is slightly closer to one without the correlated spectral function at 0.57.

Figures 2 and 3 show the E_m distribution for the four kinematics. The data points are represented in black and the data error is the sum in quadrature of the statistical and systematic errors). The blue band represents the prediction of the theoretical model with width of the band being the systematic error on the theoretical model. Most data points fit well with respect to the model with the biggest discrepancy in kinematic one at lower E_m values.

The total spectroscopic strengths using all priors and not using the spectroscopic factors from the p_m fit in Table V match within uncertainty at 20.72 ± 0.78 and 20.76 ± 1.05, respectively. The total spectroscopic strength without the correlated spectral function at 19.10 ± 0.59 does not quite matches within uncertainty but is close. The reduced χ^2 value is closest to 1 using all priors at 0.95. All of the peak energy positions and their widths match within uncertainty when using and when not using the values from the p_m fit.

TABLE IV. Comparison of the results of the χ^2 minimization using the missing momentum distributions, obtained with and without the correlated spectral function. For every state α, the extracted spectroscopic factor S_α, and its occupation number in the independent-particle shell model, N_α are presented. Additionally,the total spectroscopic strength, the number of degrees of freedom (d.o.f.), and the reduced χ^2 value are provided.

		w/ corr.	w/o corr.
α	N_α	S_α	
$1f_{7/2}$	2	0.83 ± 1.17	0.78 ± 1.35
$1d_{3/2}$	4	1.17 ± 0.22	1.34 ± 0.10
$2s_{1/2}$	2	2.02 ± 0.08	2.18 ± 0.08
$1d_{5/2}$	6	2.34 ± 1.34	2.34 ± 3.72
$1p_{1/2}$	2	2.46 ± 0.27	2.71 ± 1.19
$1p_{3/2}$	4	5.46 ± 1.69	5.46 ± 0.05
$1s_{1/2}$	2	2.17 ± 0.09	2.51 ± 0.08
corr.	0	1.20 ± 0.09	excluded
$\sum_\alpha S_\alpha$		22.16 ± 5.31	20.17 ± 4.14
d.o.f.		675	676
χ^2/d.o.f.		0.49	0.57

IV. CONCLUSIONS

We analyzed the titanium-48 data from experiment E12-14-012 at JLab and fitted the resulting spectral functions against a MC simulation as functions of p_m and E_m. We found the spectroscopic factors and the respective total spectroscopic strengths for $P(p_m)$ and $P(E_m)$, as well as the peak energy positions and their distribution widths, with great precision. The p_m fit showed no significant difference between using and not using the correlated spectral function which suggests that there is no large bias. The reduced χ^2 value is slightly closer to one at 0.57 when not using the correlated spectral function, so the fit is better. However, it is still either over fitted or the error is overestimated. The overlap of kinematics two and three in p_m,

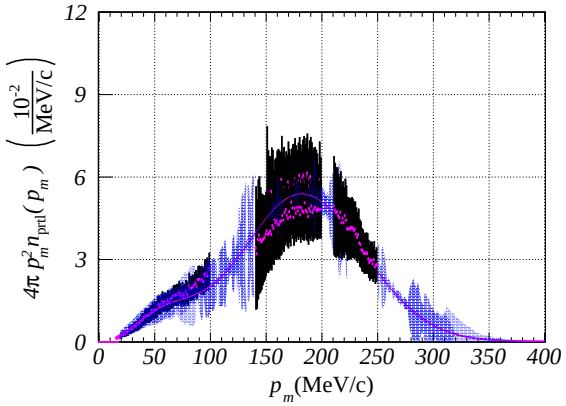

(a) $0 < E_m < 30$ MeV

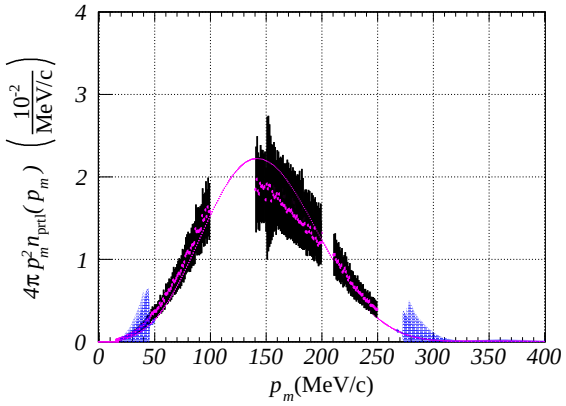

(b) $30 < E_m < 54$ MeV

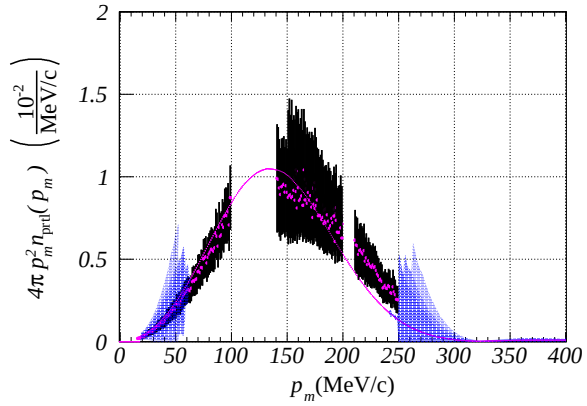

(c) $54 < E_m < 90$ MeV

FIG. 1. Partial momentum distribution obtained by integrating the test spectral function over the missing energy range of (a) 0–30 MeV, (b) 30–54 MeV, and (c) 54–90 MeV, presented with the geometric factor of $4\pi p_m^2$.

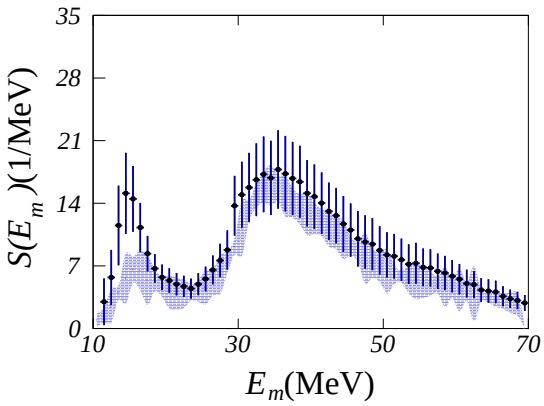

(a) $15 < p_m < 140$ MeV/c

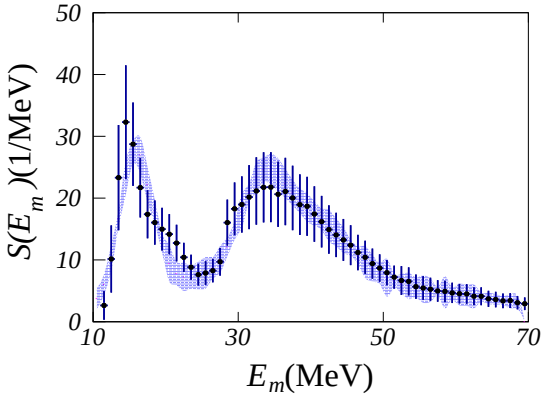

(b) $130 < p_m < 260$ MeV/c

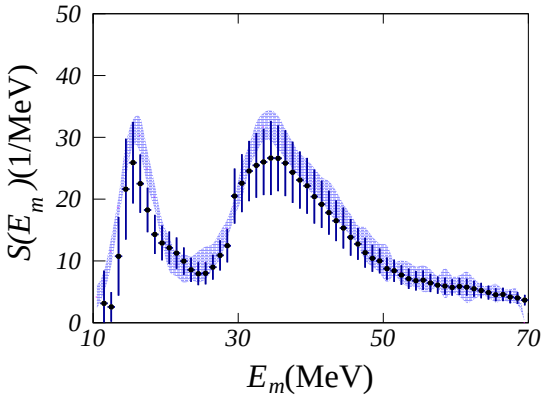

(c) $150 < p_m < 260$ MeV/c

FIG. 2. Missing energy distributions obtained for the kinematic settings of Table I. The blue band shows the results of our fit including the full error budget.

even though they have different $T_{p'}$, shows that the FSI corrections used are reliable. For the E_m fit, we found no significant difference between using all priors and not using the spectroscopic factors from the p_m fit. There was a slight difference to not using the correlated spectral function but the values are still similar indicating that there is no large bias. The fit is best

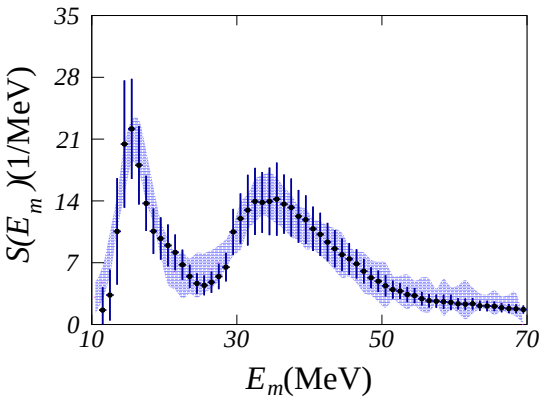

(a) $170 < p_m < 300$ MeV/c

FIG. 3. Continued from Fig. 2.

TABLE V. Comparison of the results of the χ^2 minimization using the missing energy distributions, obtained with all priors, without priors from the missing-momentum fits, and without the correlated spectral function. For every state α, the extracted spectroscopic factor S_α, and its occupation number in the independent-particle shell model, N_α are presented. Additionally,the total spectroscopic strength, the number of degrees of freedom (d.o.f.), and the reduced χ^2 are provided.

		all priors	w/o p_m	w/o corr.
α	N_α		S_α	
$1f_{7/2}$	2	1.53 ± 0.25	1.55 ± 0.28	1.24 ± 0.22
$1d_{3/2}$	4	2.79 ± 0.37	3.15 ± 0.54	3.21 ± 0.37
$2s_{1/2}$	2	2.00 ± 0.11	1.78 ± 0.46	2.03 ± 0.11
$1d_{5/2}$	6	2.25 ± 0.16	2.34 ± 0.19	3.57 ± 0.29
$1p_{1/2}$	2	2.00 ± 0.20	1.80 ± 0.27	2.09 ± 0.19
$1p_{3/2}$	4	2.90 ± 0.20	2.92 ± 0.20	4.07 ± 0.15
$1s_{1/2}$	2	2.14 ± 0.10	2.56 ± 0.30	2.14 ± 0.11
corr.	0	1.07 ± 0.07	0.96 ± 0.11	excluded
$\sum_\alpha S_\alpha$		20.72 ± 0.78	20.76 ± 1.05	19.10 ± 0.59
d.o.f		121	153	125
χ^2/d.o.f.		0.95	0.71	1.23

TABLE VI. The peak positions E_α, their widths σ_α, and the parameter E_{corr} of the correlated spectral function obtained from the χ^2 minimization of missing energy distributions. The results with and without priors from the missing momentum fit are compared.

	E_α (MeV)		σ_α (MeV)	
α	w/ priors	w/o priors	w/ priors	w/o priors
$1f_{7/2}$	11.32 ± 0.10	11.31 ± 0.10	8.00 ± 5.57	8.00 ± 6.50
$1d_{3/2}$	12.30 ± 0.24	12.33 ± 0.24	7.00 ± 0.61	7.00 ± 3.84
$2s_{1/2}$	12.77 ± 0.25	12.76 ± 0.25	7.00 ± 3.76	7.00 ± 3.84
$1d_{5/2}$	15.86 ± 0.20	15.91 ± 0.22	2.17 ± 0.27	2.23 ± 0.29
$1p_{1/2}$	33.33 ± 0.60	33.15 ± 0.65	3.17 ± 0.45	3.03 ± 0.48
$1p_{3/2}$	39.69 ± 0.62	39.43 ± 0.68	5.52 ± 0.70	5.59 ± 0.70
$1s_{1/2}$	53.84 ± 1.86	52.00 ± 3.13	11.63 ± 1.90	13.63 ± 2.59
corr.	25.20 ± 0.02	25.00 ± 0.29	—	—

when using all priors with a reduced χ^2 value of 0.95. Overall, the data is in good agreement with the theoretical model. Provided (e,e′p) scattering in titanium can be shown to be a good model for (e,e′n) in argon, this data can be used for precise measurements in neutrino experiments like DUNE.

ACKNOWLEDGMENTS

I would like to thank my mentor, Prof. Camillo Mariani, for his help and guidance. I acknowledge the outstanding support from the National Science Foundation, the Virginia Tech Physics department and the Virginia Tech Center for Neutrino Physics. This work was made possible by the National Science Foundation under grant No. PHY−2149165.

[1] B. Abi, *et al.*, (The DUNE Collaboration), Journal of Instrumentation **15**, T08008 (2020).

[2] https://www.dunescience.org/.

[3] https://lbnf-dune.fnal.gov/.
[4] C. Barbieri, Rocco, and V. Somà, Phys.Rev. C **100**, 062501(R) (2019).
[5] O. Benhar, C. Mariani, C.-M. Jen, D. B. Day, D. Higinbotham *et al.*,Proposal to the Jefferson Lab Program Advisory Committee PAC 42 (2014).
[6] T. de Forest Jr., Nucl. Phys. A **392**, 232 (1983).
[7] A. E. L. Dieperink, T. de Forest Jr., I. Sick, and R. A. Brandenburg, Phys. Lett. B **63**, 261 (1976).
[8] SIMC Monte Carlo, https://hallcweb.jlab.org/wiki/index.php/SIMC_Monte_Carlo.
[9] J. Chen, Nucl. Data Sheets **149**, 1 (2018).
[10] G. Mairle, M. Seeger, H. Reinhardt, T. Kihm, K. T. Knöpfle, and Chen Lin Wen, Nucl. Phys. A **565**, 543 (1993).
[11] Meng Wang, G. Audi, F. G. Kondev, W. J. Huang, S. Naimi, and Xing Xu, Chin. Phys. C **41**, 030003 (2017).
[12] G. Mairle, Phys. Lett. B **304**, 39 (1993).
[13] L. Jiang *et al.* [Jefferson Lab Hall A], Phys. Rev. D **105**, 112002.
[14] F. James, "MINUIT Function Minimization and Error Analysis: Reference Manual Version 94.1," CERN-D-506.
[15] R. Brun and F. Rademakers, Nucl. Instrum Methods Phys. Res. A **389**, 81 (1997).